Research Article

Amperometric H_2O_2 sensor based on gold nanoparticles/poly (celestine blue) nanohybrid film

N. S. Sangeetha[1,2] · S. Sriman Narayanan[2]

Abstract
The present paper demonstrates a significant hybrid nanofilm using gold nanoparticles (GNPs) and poly celestine blue (PCB) as an effective sensing material for hydrogen peroxide (H_2O_2). The surface assembly of the nanocatalyst GNPs provides greater surface area for improved layering of PCB on the electrode surface. Cyclic voltammetry, UV visible spectroscopy and field emission scanning electron microscopy studies confirmed the structure and morphology of the synthesized GNPs. Cyclic voltammetric characterization of the fabricated GNPs/PCB electrode was performed and under optimal conditions they exhibited enhanced electrochemical sensing towards H_2O_2 with better sensitivity and detection limit as 0.22 µA/µM and 3.9×10^{-6} M (S/N = 3). The interference studies using the GNPs/PCB modified electrode interprets the selectivity of the electrode towards H_2O_2. The proposed sensor was highly stable and was effectively applied for analysis of H_2O_2 in real samples.

Keywords Poly (celestine blue) · Gold nanoparticles · Hydrogen peroxide · Amperometry · Nanomaterial · Sensor

1 Introduction

The development of electrochemical sensors has become one of the most promising research areas mainly due to its potential applications in the development of analytical devices. The designing of these amperometric sensors with better analytical abilities has led to the discovery of nano structured materials with high surface area especially inorganic metal nanoparticles (MNPs). In electrochemistry, gold nanoparticles (GNPs), have found a wide range of applications in electroanalysis [1], bioelectroanalysis [2] and electrocatalysis [3]. Among the several MNPs, GNPs are distinctively advantageous as it offers a stable platform for efficient immobilization of redox mediators and bio molecules thereby retaining the electrochemical activity of the immobilized molecules [4]. Its effective biocompatabiltiy has increased the research interest in GNPs based biosensors [5]. A large number of studies have shown that the GNPs based sensors enhance the electrode conductivity, facilitate the electron transfer and improve the detection limit of bio molecules [6, 7].

Incorporation of several organic dyes as redox mediators on the electrode surface is receiving considerable interest due to their high electron transfer efficiency and cost effectiveness. These dye molecules are immobilized on the electrode surface by various techniques like adsorption [8], direct electropolymerization [9], cross-linking methods [10] and sol–gel techniques [11]. The conducting dye polymers have received great attention due to their good reproducibility providing more active sites and homogeneity. Even though the electropolymerization is a preferred technique for immobilizing the polymers, controlling the film thickness, charge transport features and the electrochemical stability of polymer film formed still remains to be a question. Based on the various studies on the characteristics and

✉ S. Sriman Narayanan, sriman55@yahoo.com | [1]Department of Chemistry, Bhaktavatsalam Memorial College for Women, Korattur, Chennai, Tamil Nadu 600 080, India. [2]Department of Analytical Chemistry, School of Chemical Sciences, University of Madras, Guindy Campus, Chennai, Tamil Nadu 600 025, India.

SN Applied Sciences (2019) 1:732 | https://doi.org/10.1007/s42452-019-0651-9

Received: 6 March 2019 / Accepted: 19 May 2019 / Published online: 17 June 2019

applications of nano matrix providing better electrochemical sensing and stability, we attempt to integrate the conducting dye polymer PCB on the GNPs modified electrodes.

Hydrogen peroxide (H_2O_2) is an important by product of enzymatic oxidation of several highly selective oxidases. H_2O_2 plays a major role in the metabolism of proteins, carbohydrates, fats etc. and also helps in regulation of blood sugar and in cellular energy production. Moreover the powerful oxidizing property of H_2O_2 and its derivatives has found them extensive applications in the synthesis of many organic compounds. Therefore the detection of H_2O_2 has gained vital importance in environmental, clinical and pharmaceutical analyses [12]. Various analytical methods have been developed for the determination of H_2O_2 including titrimetry [13], spectrophotometry [14], spectrofluorometry [15], chemiluminescence [16], high performance liquid chromatography [17] and electrochemistry [18]. Owing to the difficulties of these methods like interference effects and time consumption, the electrochemical methods are found to be more reliable due to their fast detection and high selectivity and sensitivity [19]. The direct oxidation or reduction of H_2O_2 at ordinary solid electrodes requires a large over potential which can be efficiently overcome by modifying the bare electrode with suitable electrocatalysts [20, 21]. Studies have shown that the electrodes modified with carbon nanotubes [22], metal alloys [23], and metal oxides [24] exhibit good catalytic activity for direct electrochemistry of H_2O_2. Enzymeless H_2O_2 sensors using various promising materials along with silver nanoparticles like reduced graphene oxide [25, 26], poly (m-phenylenediamine) microparticle [27], polypyrrole colloids [28], poly aniline nanofibers [29], graphene nanocomposites [30], Te Oxide nanowires [31] have been reported. On comparing the electrochemical behaviour of the above electrodes, it has been evident that GNPs show good catalytic activity toward H_2O_2 reduction.

Previously, we have reported PCB modified electrodes based on carbon nanotubes and graphene oxide for the detection of H_2O_2 [32, 33]. Herein, in the present work, we have fabricated an amperometric H_2O_2 sensor by electropolymerizing PCB on GNPs modified electrode. The electrochemical properties of the GNPs/PCB modified electrode have been evaluated by cyclic voltammetry and the surface morphology was examined by FESEM analysis. The electrocatalytic activity of the modified electrode for the reduction of H_2O_2 has also been investigated. The analytical utilities have been explored by using the GNPs/PCB modified electrode for amperometric and real sample detection of hydrogen peroxide. We also report the electrochemical performance and the stability of the developed electrode with high reproducibility and repeatability.

2 Experimental

2.1 Chemicals and apparatus

Analytical grade chemicals were used for all the electrochemical determinations. Hydrogen peroxide (H_2O_2) was purchased from Merck, India. Celestine blue and Chloro auric acid were purchased from Sigma Aldrich, USA. 0.1 M NH_4NO_3 was employed as the supporting electrolyte. The pH value was adjusted with PBS (0.1 M). All the solutions were prepared using double distilled water.

All the electrochemical measurements were performed in CHI 660B electrochemical workstation (CH Instruments, USA) provided with standard three electrode configuration. The saturated calomel electrode was taken as the reference electrode and the platinum electrode as auxiliary. Graphite electrode (3 mm diameter) modified with GNPs and PCB was used as working electrode. The electrolyte solution was purged with pure nitrogen to remove dissolved oxygen before the experiment. Transmission electron microscopic (TEM) images were obtained using Hitachi, H7650 Microscope. The surface morphology of GNPs/PCB and GNPs modified electrodes were observed on a SU6600 field emission scanning electron microscopy (FE-SEM) (HITACHI, Japan), equipped with an energy-dispersive X-ray analyzer at an accelerating voltage of 30 kV. pH measurements were made with Elico pH meter (model LI 120).

2.2 Preparation and characterization of gold nanoparticles (GNPs)

The citrate capped gold nanoparticles were prepared by a process reported earlier [34]. The electrochemical characterization of GNPs exhibited a typical quasi-reversible redox behaviour corresponding to the oxidation and reduction of GNPs as shown in Fig. 1a [35]. The UV analysis confirmed the synthesized GNPs as the absorption maximum was observed at 520 nm (Fig. 1b). Moreover the TEM study (Fig. 1c) was also employed to study the morphology of GNPs. The GNPs with a particle size of 5–10 nm were obtained with slight agglomeration.

2.3 Electrode fabrication

The fabrication methodology of GNPs/PCB modified electrode involved the electropolymerisation of Celestine blue on GNPs modified graphite electrode. The electropolymerization process was carried out using cyclic voltmmetry. The procedure is as follows: 5 µL of GNPs was dropcasted on the polished graphite electrode surface and then dried.

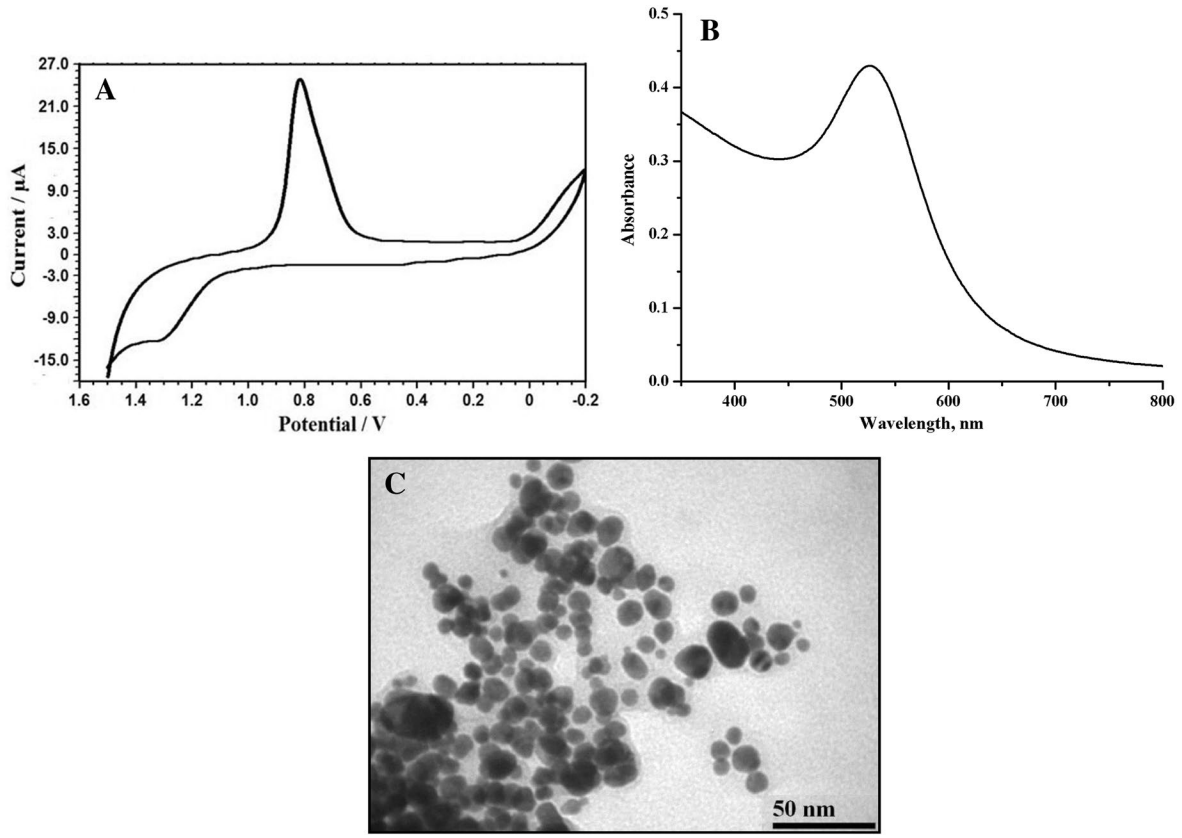

Fig. 1 **a** CVs of GNPs drop casted on graphite electrode in 0.1 M H_2SO_4 at 100 mV/s, **b** UV–Vis spectra, **c** TEM analysis of synthesized GNPs

PCB was electrodeposited on the GNPs modified electrode from a solution of 3 mM of celestine blue in 0.05 M NH_4NO_3 (scan rate of 50 mV/s). The fabrication of GNPs/PCB modified electrode is shown in the scheme 1. GNPs modified graphite electrode and PCB modified graphite electrode were also prepared for comparing the effective electrochemical and electrocatalytic behaviour of GNPs/PCB modified electrodes.

3 Results and discussion

3.1 FESEM and EDS analysis

The topographical analysis by FESEM and EDS studies for the fabricated GNPs and GNPs/PCB modified electrodes exhibited a uniform dispersion of GNPs (5–10 nm) on the electrode surface with negligible aggregation (Fig. 2a). The PCB appeared as a cloudy layer over the GNPs on the electrode (Fig. 2c). The above results were further confirmed by the elemental analysis (Fig. 2b, d). Moreover the presence of GNPs provides a higher surface area for efficient immobilization of PCB thereby enhancing the electrocatalytic activity of the mediator.

3.2 Electrochemical characterization

To evaluate the influence and to study the electrochemical compatibility of the GNPs/PCB modified electrode, CVs were recorded in the presence of various supporting electrolytes like $NaNO_3$, K_2SO_4, NaCl, LiCl, NH_4NO_3 of 0.1 M concentration. Well defined redox waves (Fig. 3)

Scheme 1 Fabrication of GNPs/PCB modified electrode

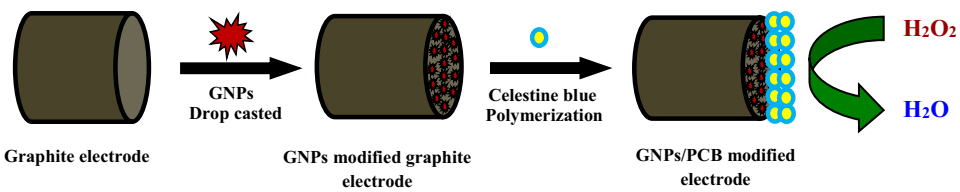

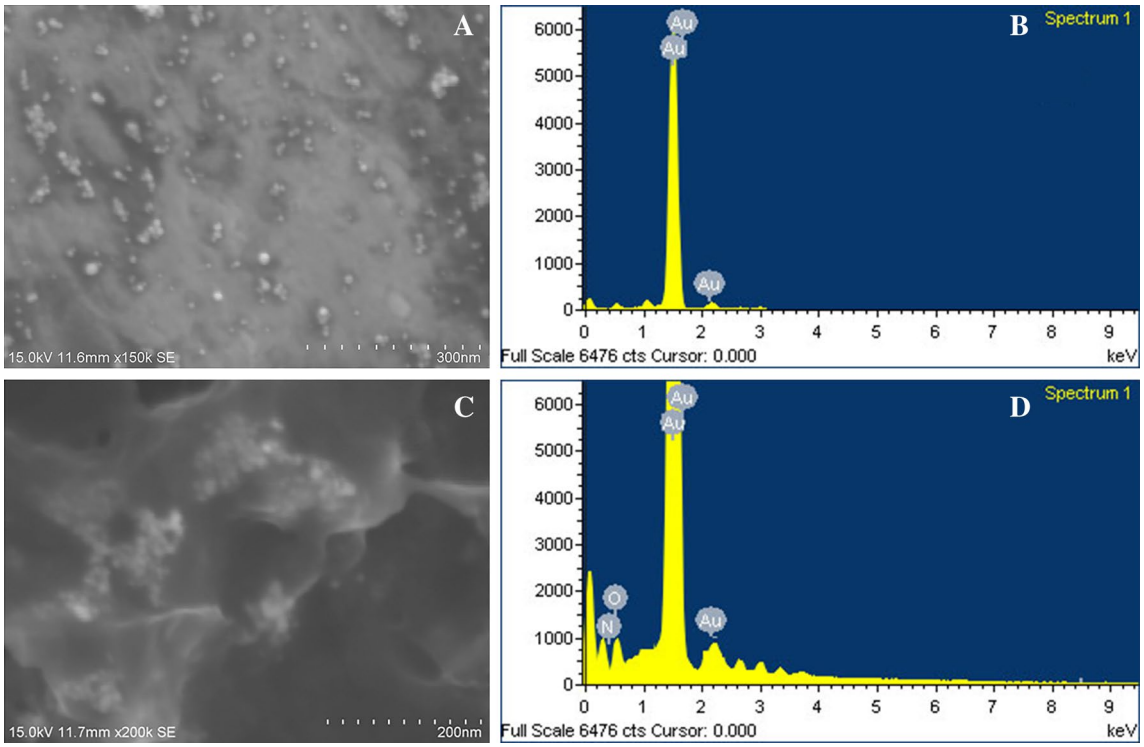

Fig. 2 FESEM and EDS images of GNPs (**a**, **b**) and poly (celestine blue) on GNPs modified electrode (**c**, **d**)

were recorded in the presence of NH_4NO_3 (0.1 M) as electrolyte which is attributed to their favourable electron transfer conditions. The voltammograms obtained with other electrolytes were ill defined. Hence this enabled us to choose NH_4NO_3 (0.1 M) solution as the background electrolyte for subsequent studies. The pH rapport of GNPs/PCB modified electrode was also studied in the pH range of 3–10. The results clearly displayed an increased current response at pH 7 (not shown). So pH 7 was maintained for all the electrochemical measurements by using 0.05 M PBS buffer solution along with 0.1 M NH_4NO_3.

To explain the electrochemical performance of the GNPs/PCB modified electrodes, comparative cyclic voltammetric responses along with GNPs and PCB modified electrodes are given in Fig. 4a. Curves a. b, c and d (Fig. 4a) corresponds to the voltammograms of bare, GNPs, PCB and GNPs/PCB modified electrode in 0.1 M NH_4NO_3 (pH 7) at a scan rate of 50 mV/s. A pair of oxidation and reduction peaks occurs at − 0.15 V and − 0.34 V for the GNPs/PCB modified electrode (curve d) with a formal potential of − 0.24 V. Higher peak currents were recorded for GNPs/PCB modified electrode when compared with PCB modified electrode. This exhibits well resolved nerstian behaviour of GNPs/PCB electrode rather than the electrodes without GNPs. This response is due to the fact that GNPs can highly facilitate the electron transfer of PCB.

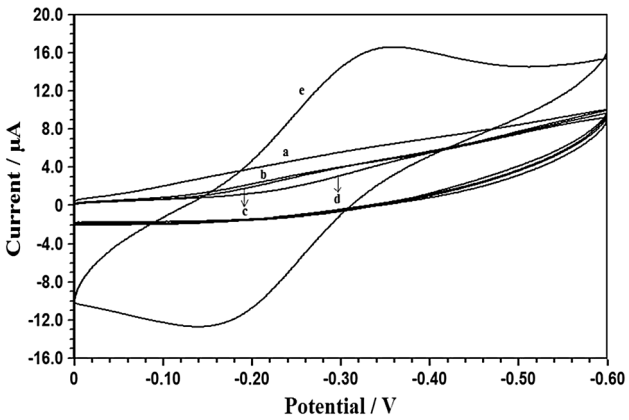

Fig. 3 CVs of GNPs/PCB modified electrode in the presence of 0.1 M (a) $NaNO_3$ (b) K_2SO_4 (c) NaCl (d) LiCl (e) NH_4NO_3, Scan rate: 50 mV/s

3.3 Scan rate variation

Figure 4b shows the effect of scan rate on the peak currents. As can be seen, a linear increase in current with increasing scan rate was recorded in the range 2–150 mV/s with a slight shift in the peak potential. This behaviour represents a surface-controlled process. Moreover a good linearity and correlation coefficient (0.99—cathodic and 0.9857—anodic) was exhibited when a calibration graph of scan rate against peak currents was plotted. The surface

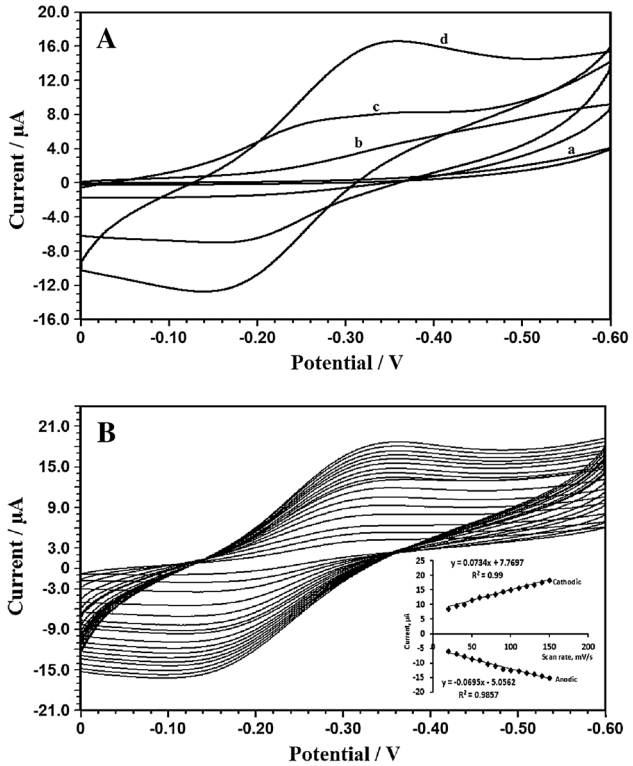

Fig. 4 **a** CVs of (a) bare (b) GNPs (c) PCB and (d) GNPs/PCB modified electrode, Scan rate: 50 mV/s **b** CVs of GNPs/PCB modified electrode at different scan rates; Inset: Dependence of peak current versus scan rate. Electrolyte: 0.1 M NH_4NO_3 (pH 7)

coverage of GNPs modified and bare graphite electrode with PCB was calculated using the equation,

$$C = Q/nFA$$

where Q represents the anodic or cathodic charge under the peak in coulombs, F is the Faraday constant (96,485 C mol^{-1}), A is the surface area of the electrode and n is the number of electrons transferred [36]. The calculated Γ values for GNPs/PCB modified graphite electrode was 4.87×10^{-10} mol/cm^2 and that of PCB modified electrode was recorded as 1.69×10^{-10} mol/cm^2. The differences in the Γ values indicate that the GNPs have provided stable and a higher surface area for the efficient growth of PCB film.

3.4 Electro catalytic reduction of H_2O_2

The electrocatalytic activity of GNPs/PCB modified electrode was studied in 0.1 M NH_4NO_3 (pH 7) containing desired concentration of H_2O_2 at a scan rate of 50 mV/s. Figure 5a compares the CVs of bare graphite, PCB electrode, GNPs/PCB modified electrode in the absence (curve a, c, e) and in the presence (curve b, d, f) of 8.26×10^{-5} M H_2O_2. From the CVs it is observed that the bare graphite and PCB modified electrode (curve b, d) exhibited weak reduction currents at very high potentials. But with the GNPs/PCB modified electrode in the presence of H_2O_2 a predominant increase in the reduction current was observed. This increase in the current response of GNPs/PCB modified electrode on comparison with PCB modified electrode can be designated due to the synergistic effect of GNPs. The reduction current was found to increase linearly with increasing H_2O_2 concentration (Fig. 5b). The enhancement in the reduction current can be ascribed to the electro catalytic effect of the PCB. At the applied potential, the oxidised form of the PCB on the electrode surface gets reduced. This reduced form of PCB further reduces H_2O_2 and in turn gets oxidized. This behaviour of PCB is invariably amplified by the presence of GNPs on the electrode surface as discussed earlier. Based on the results observed, the possible catalytic mechanism of H_2O_2 reduction and PCB regeneration is given below.

$$PCB_{(Oxd)} \longrightarrow 2H^+ + 2e^- PCB_{(Red)}$$

$$PCB_{(Red)} + H_2O_2 \underset{\text{Reduction}}{\overset{\text{Catalytic}}{\longleftrightarrow}} \underset{\text{(Regenerated)}}{PCB_{(Oxd)}} + 2H_2O$$

As depicted in the calibration graph (Fig. 5b inset) plotted between catalytic current and H_2O_2 concentration, the GNPs/PCB modified electrode was able to effectively eelctrocatalyse H_2O_2 in the linear concentration range from 1.17×10^{-5} M to 1.29×10^{-3} M ($R^2=0.9998$). The detection limit and sensitivity was calculated as 3.9×10^{-6} M (S/N = 3) and 0.22 µA/µM respectively. The RSD obtained was 1.5% for ten repetitive additions of 3.23×10^{-4} M of H_2O_2. The effect of the solution pH on the catalytic behavior of GNPs/PCB modified electrode was studied in the range of 3–10. Figure 6a shows the effect of pH on the reduction peak current of GNPs/PCB modified electrode in the presence of 3.23×10^{-4} M H_2O_2. At pH values lesser than 5 (acidic medium), no appreciable change in the peak currents were observed. A maximum current response at lower potential was recorded at pH 7. The electrocatalytic signal was found to decrease above pH 7 which may be due to the minor dissolution of the mediator in the alkaline medium. This implies that the electro catalytic property of PCB depend greatly on solution pH.

The electrochemicalal reduction ability of the as prepared GNPs/PCB modified electrode towards H_2O_2 detection was further examined by performing DPV studies. Figure 6b shows the DPV response of GNPs/PCB modified electrode towards increasing concentration of H_2O_2 in 0.1 M NH_4NO_3. It was evident that there was a proportional increase in the peak current with respect to the concentration of H_2O_2 added. This is indicated by the linearity ($R^2=0.969$) obtained in the calibration plot (Fig. 6b Inset) between the concentration of H_2O_2 and the so obtained

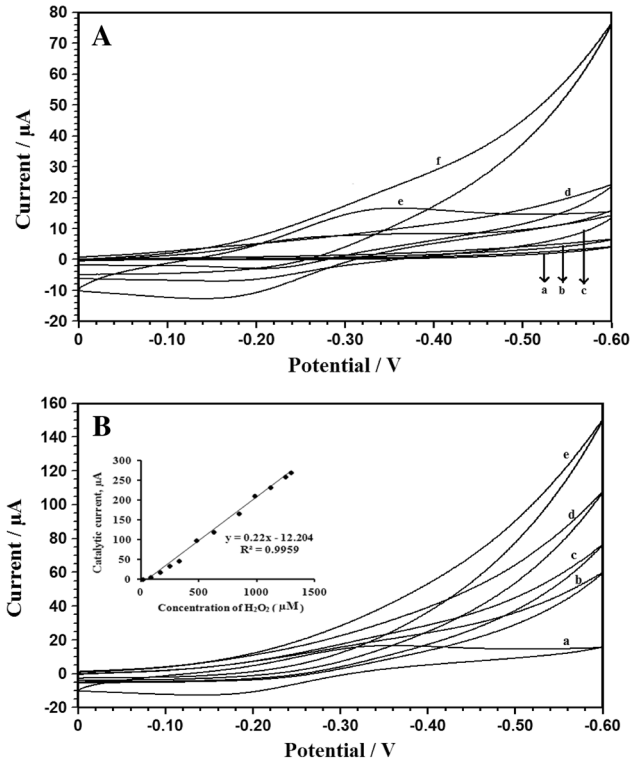

Fig. 5 **a** CVs of bare, PCB and GNPs/PCB modified electrode in the absence (a, c, e) and presence (b, d, f) of 8.26×10^{-5} M H_2O_2. **b** Peak current response of GNPs/PCB modified electrode for successive additions of H_2O_2; Inset: Calibration plot of catalytic current versus concentration of analyte. **b** Effect of pH for the peak current response of GNPs/PCB modified electrode in presence of 3.23×10^{-4} M of H_2O_2. Electrolyte: 0.1 M NH_4NO_3 (pH 7), Scan rate: 50 mV/s

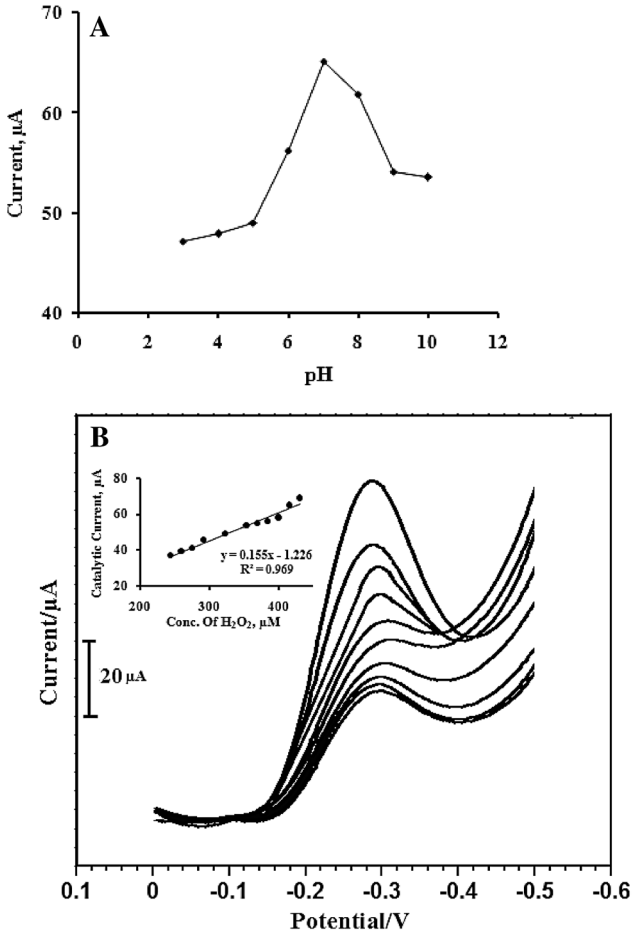

Fig. 6 **a** Effect of pH for the peak current response of GNPs/PCB modified electrode in presence of 3.23×10^{-4} M of H_2O_2. Electrolyte: 0.1 M NH_4NO_3 (pH 7), Scan rate: 50 mV/s. **b** DPV response of GNPs/PCB modified electrode for the successive additions of 0.1 ml of 0.01 M H_2O_2; Inset: Calibration plot of catalytic current versus concentration of H_2O_2

catalytic current. This reveals the electro catalytic sensing accuracy of the GNPs/PCB modified electrodes towards detection H_2O_2.

3.5 Amperometric determination of H_2O_2

To investigate the applicability of the GNPs/PCB modified electrode towards H_2O_2 determination under dynamic conditions, hydrodynamic voltmmetry analysis (HDV) was performmed. The HDVs were recorded in the presence of 3.23×10^{-4} M H_2O_2 for the bare and GNPs/PCB modified electrode (Fig. 7a) in the range of 0 to − 0.7 V at a stirring rate of 300 rpm. The peak currents of the modified electrode (curve b) increased with increasing potential with a maximum response at of − 0.35 V. The bare electrode (curve a) did not show any considerable current response at the same potential and was found to detect H_2O_2 at higher potential with least sensitivity. So an optimal operational potential of − 0.35 V was fixed for the chronoamperometric determination.

Figure 7b illustrates the chronoamperometric response of the GNPs/PCB modified electrode for successive additions of 0.5 ml of 0.01 M H_2O_2 in 0.1 M NH_4NO_3 at a constant potential of − 0.35 V. The steady state was reached within 4 s with a rapid increase in the current after each addition. The inset in Fig. 7b gives the calibration plot between the catalytic current response and time. A linear response within the concentration range of 8.26×10^{-5} M to 1.04×10^{-3} M (under study) with a correlation co efficient of 0.995 was obtained.

This highlights the high catalytic sensitivity of the electrode under dynamic conditions. A comparison of the present GNPs/PCB modified electrode towards the determination of H_2O_2 with other sensors is tabulated in Table 1.

3.6 Effect of interferents

The selectivity of the GNPs/PCB modified electrodes in the electrochemical determination of H_2O_2 in the presence of various analytes like ascorbic acid, uric acid and acetic acid was analysed. The interfering species were chosen on the basis of their co existence with H_2O_2 in biological and food samples. The influence of the three interferants (82 µM) was monitored amperometrically under optimized parameters by applying a constant potential of − 0.35 V (Fig. 8). Ascorbic acid, uric acid and acetic acid were added at regular intervals of time in the presence of 2.43×10^{-4} M of H_2O_2. As evident from Fig. 8, there was no additional current response on subsequent injection of these analytes. The low potential determination of H_2O_2 excludes the interference effects indicting the high degree of selectivity of the GNPs/PCB modified electrodes.

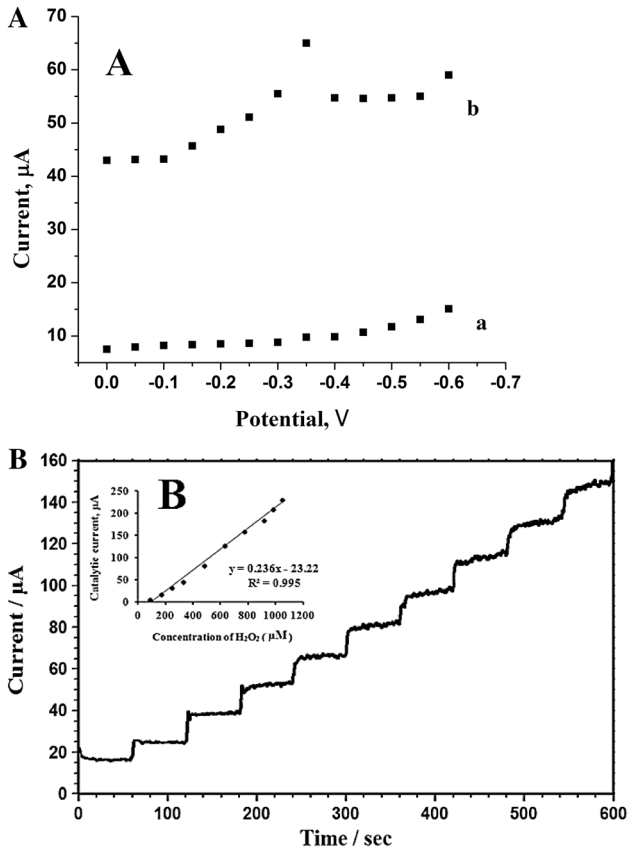

Fig. 7 **a** Hydrodynamic voltammograms of (a) bare (b) GNPs/PCB modified electrode in presence of 3.23×10^{-4} M of H_2O_2, **b** chronoamperometric response for H_2O_2 at GNPs/PCB modified electrode for each 0.5 ml addition of 0.01 M H_2O_2. Inset: Calibration graph; Fixed potential: -0.35 V; Electrolyte: 0.1 M NH_4NO_3 solution (pH 7), Scan rate: 50 mV/s under stirring condition

3.7 Real sample analysis

The determination of H_2O_2 in milk samples was carried to verify the practical application of the GNPs/PCB modified sensor. The analysis was carried out with two different branded milk samples. For this purpose, 5 ml of the boiled milk was filtered and diluted to ten times and used for electrochemical determinations. Initially a blank milk sample was tested. No characteristic signal was observed which confirmed the absence of H_2O_2. The sample was then spiked with two different concentrations of H_2O_2 and the recoveries were calculated. The H_2O_2 concentration determined in the samples using our method is listed in Table 2. Furthermore, the desirable recovery of H_2O_2 in the milk samples by GNPs/PCB modified electrode verifies the suitability of the proposed sensor for real sample analysis.

3.8 Stability and reproducibility

The stability of the GNPs/PCB modified electrode was also studied. The electrode was subjected to 100 continuous cycles at a scan rate of 50 mV s^{-1} in 0.1 M NH_4NO_3

Table 1 Comparison of the present GNPs/PCB modified electrode with other H_2O_2 sensors

Electrode	Linear range (µM)	LOD (µM)	References
Pd[a]Cu[b]/SPCE[c]	500–11,000	0.7	[37]
N-graphene-Ag NDs[d]/ITO[e]	100–80,000	0.26	[38]
Cu_2O[f]	300–1280	2.6	[39]
Co_3O_4[g]/MWCNTS[h]	20–430	2.46	[40]
s-SPE[i]/ODA[j]-rGO[k]-ODA[j]-PB[l]	5–1000	2	[41]
Silver nanowire array	100–3100	29.2	[42]
GNPs[m]/PCB[n]	11.7–1290	3.9	Present work

[a]Palladium
[b]Copper
[c]Screen printed carbon electrodes
[d]Silver nanodendrites
[e]Indium tin oxide
[f]Cuprous oxide
[g]Cobalt oxide
[h]Multiwalled carbon nanotubes
[i]Screen printed eelctrodes
[j]Octadecylamine
[k]Reduced graphene oxide
[l]Prussian blue
[m]Gold nanoparticles
[n]Poly celestine blue

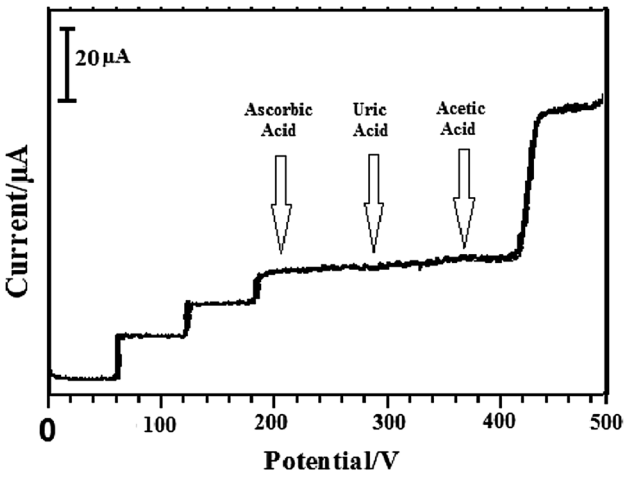

Fig. 8 Chronoamperometric response on successive additions of 82 µM Ascorbic acid, Uric acid and Acetic acid in the presence of 2.43×10^{-4} M of H_2O_2; Fixed potential: −0.35 V; Electrolyte: 0.1 M NH_4NO_3 solution (pH 7), Scan rate: 50 mV/s under stirring condition

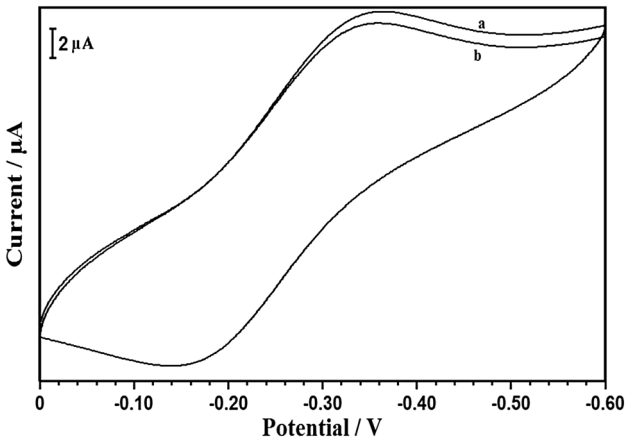

Fig. 9 Cyclic voltammograms of **a** 1st and **b** 100th cycle of GNPs/PCB modified electrode in 0.1 M NH_4NO_3, Scan rate: 50 mV s^{-1}. Electrolyte: 0.1 M NH_4NO_3 (pH 7), Scan rate: 50 mV/s

Table 2 Determination of H_2O_2 in milk sample

Sample No	Added (10^{-4} M)	Found (10^{-4} M)	Recovery (%)
1	5	4.98	99.6
	10	9.97	99.7
2	5	4.99	99.8
	10	100.1	100.1

(pH 7) (Fig. 9). The current response remained unaffected between the 1st and the 100th cycle. The studies depicted that the current response of GNPs/PCB modified electrode in the presence of H_2O_2 and the catalytic currents for the reduction of H_2O_2 were effectively reproducible. Electropolymerization of the celestine blue on the GNPs modified electrode forms a stable redox active layer and also retains the catalytic ability of the GNPs. This confirms that the proposed electrochemical sensor is highly stable and can be repeatedly used with reserved performance.

4 Conclusion

The present study has resulted in a unique fabrication approach of GNPs/PCB electrochemical sensor by electropolymerization of celestine blue on GNPs coated electrode. The GNPs synthesized were characterized by UV and TEM studies confirming the particle size in the range of 5–10 nm. The presence of GNPs enhanced the surface area for effective adsorption of the polymerized dye molecule facilitating electron transfer and thereby also enhances the stability of the sensor. The fabricated GNPs/PCB sensor exhibited effective electrocatalytic activity and amperometric response towards H_2O_2 determination with detection limit, linear concentration range and sensitivity as 3.9×10^{-6} M (S/N = 3), 1.17×10^{-5} M to 1.29×10^{-3} M and 0.22 µA/µM respectively. The present GNPs/PCB modified electrodes was successfully applied for the detection of H_2O_2 in milk samples with reliability and reproducibility.

Acknowledgements The authors gratefully acknowledge the Department of Science and Technology, New Delhi for financial assistance through PURSE Program.

Complice with ethical standards

Conflict of interest On behalf of all the authors, the corresponding author states that there is no conflict of interest.

References

1. Katz E, Willner I, Wang J (2004) Electroanalytical and bioelectroanalytical systems based on metal and semiconductor nanoparticles. Electroanalysis 16:19–44
2. Fang Y, Xu Y, He PJ (2005) DNA biosensors based on metal nanoparticles. Biomed Nanotechnol 1:276–285
3. Wildgoose GG, Banks CE, Compton RG (2006) Metal nanoparticles and related materials supported on carbon nanotubes: methods and applications. Small 2:182–193
4. Viswambari devi R, Doble M, Rama Verma S (2015) Nanomaterials for early detection of cancer biomarker with special emphasis on gold nanoparticles in immunoassays/sensors. Biosens Bioelectron 68:688–698
5. Shan C, Yang H, Han D, Zhang Q, Ivaskab NL (2010) Graphene/AuNPs/chitosan nanocomposites film for glucose biosensing. Biosens Bioelectron 25:1070–1074
6. Zhang Z, Jia J, Lai Y, Ma Y, Weng J, Sun L (2010) Conjugating folic acid to gold nanoparticles through glutathione for targeting and detecting cancer cells. Bioorg Med Chem 18:5528–5534

7. Ning R, Wenbo L, Zhang Y, Qin X, Luo Y, Jianming H, Asiri AM, Al-Youbi AO, Sun X (2012) A novel strategy to synthesize Au nanoplates and their application for enzymeless H_2O_2detection. Electrochim Acta 60:13–16
8. Ye J, Baldwin RP (1988) Catalytic reduction of myoglobin and hemoglobin at chemically modified electrodes containing methylene blue. Anal Chem 60:2263–2268
9. Malinauskas A, Ruzgas T, Gorton L (2000) Electrochemical study of the redox dyes nile blue and toluidine blue adsorbed on graphite and zirconium phosphate modified graphite. J Electroanal Chem 484:55–63
10. Lin XQ, Chen J, Chen ZH (2000) Amperometric biosensor for hydrogen peroxide based on immobilization of horseradish peroxidase on methylene blue modified graphite electrode. Electroanalysis 12:306–310
11. Zhang J, Li B, Wang Z, Chen G, Dong S (1999) Functionalized inorganic–organic composite material derivated by sol–gel for construction of mediated amperometric hydrogen peroxide biosensor. Anal Chim Acta 388:71–78
12. Alpat I, Alpat SK, Dursun Z, Telefoncu A (2009) Development of a new biosensor for mediatorless voltammetric determination of hydrogen peroxide and its application in milk samples. J Appl Electrochem 39:971–977
13. Prasada Rao MS, Mohan Rao AR, Ramana KV, Sagi SR (1990) Thallimetric oxidations -V: titrimetric and spectrophotometric determination of hydrogen peroxide. Talanta 37:753–755
14. Zhang K, Mao L, Cai R (2000) Stopped-flow spectrophotometric determination of hydrogen peroxide with hemoglobin as catalyst. Talanta 51:179–186
15. Tang B, Wang Y (2003) Spectrofluorimetric determination of both hydrogen peroxide and O–O–H in polyethylene glycols (PEGs) using 2-hydroxy-1-naphthaldehyde thiosemicarbazon (HNT) as the substrate for horseradish peroxidase (HRP). Spectrochim Acta A 59:2867–2874
16. Zhou GJ, Wang G, Xu JJ, Chen HY (2002) Reagentless chemiluminescence biosensor for determination of hydrogen peroxide based on the immobilization of horseradish peroxidase on biocompatible chitosan membrane. Sens Actuators B 81:334–339
17. Tarvin M, McCord B, Mount K, Sherlach K, Miller ML (2010) Optimization of two methods for the analysis of hydrogen peroxide: high performance liquid chromatography with fluorescence detection and high performance liquid chromatography with electrochemical detection in direct current mode. J Chromatogr A 1217:7564–7572
18. Liu S, Wang L, Tian J, Luo Y, Zhang X, Sun X (2011) Aniline as a dispersing and stabilizing agent for reduced graphene oxide and its subsequent decoration with Ag nanoparticles for enzymeless hydrogen peroxide detection. J Colloid Interface Sci 363:615–619
19. Taha Z, Wang J (1991) Electrocatalysis and flow detection at a glassy carbon electrode modified with a thin film of oxymanganese species. Electroanalysis 3:215–219
20. Daniel S, Rao TP, Rao KS, Rani SU, Naidu GRK, Lee HY, Kawai T (2007) A review of DNA functionalized/grafted carbon nanotubes and their characterization. Sens Actuators B 122:672–682
21. Guldi DM, Rahman GMA, Zerbetto F, Prato M (2005) Carbon nanotubes in electron donor–acceptor nanocomposites. Acc Chem Res 38:871–878
22. Lee D-J, Choi S-W, Byun YT (2018) Room temperature monitoring of hydrogen peroxide vapor using platinum nanoparticles-decorated single-walled carbon nanotube networks. Sens. Actuators B Chem 256:744–750
23. Kazici HC, Cagler A, Aydogmus T, Aktas N, Kiyrak H (2018) Microstructured prealloyed titanium–nickel powder as a novel nonenzymatic hydrogen peroxide sensor. J Colloid Interface Sci 530:353–360
24. Guler M, Turkoglu V, Kivrak A, Karahan F (2018) A novel nonenzymatic hydrogen peroxide amperometric sensor based on Pd@CeO_2-NH_2nanocomposites modified glassy carbon electrode. Mater Sci Eng C 90:454–460
25. Liu S, Wang L, Tian J, Luo Y, Zhang X, Sun X (2011) Aniline as a dispersing and stabilizing agent for reduced graphene oxide and its subsequent decoration with Ag nanoparticles for enzymeless hydrogen peroxide detection. J Colloid Interface Sci 363:615–619
26. Liu S, Tian J, Wang L, Sun X (2011) A method for the production of reduced graphene oxide using benzylamine as a reducing and stabilizing agent and its subsequent decoration with Ag nanoparticles for enzymeless hydrogen peroxide detection. Carbon 49:3158–3164
27. Tian J, Li H, Wenbo L, Luo Y, Wanga L, Sun X (2011) Preparation of Ag nanoparticle-decorated poly(m-phenylenediamine) microparticles and their application for hydrogen peroxide detection. Analyst 136:1806–1809
28. Qin X, Wenbo L, Luo Y, Chang G, Sun X (2011) Preparation of Ag nanoparticle-decorated polypyrrole colloids and their application for H_2O_2 detection. Electrochem Commun 13:785–787
29. Chang G, Luo Y, Wenbo L, Qin X, Asiri AM, Al-Youbi AO, Sun X (2012) Ag nanoparticles decorated polyaniline nanofibers: synthesis, characterization, and applications toward catalytic reduction of 4-nitrophenol and electrochemical detection of H_2O_2 and glucose. Catal Sci Technol 2:800–806
30. Zhang Y, Liu S, Wang L, Qin X, Tian J, Wenbo L, Chang G, Sun X (2012) One-pot green synthesis of Ag nanoparticles-graphene nanocomposites and their applications in SERS, H_2O_2, and glucose sensing. RSC Adv 2:538–545
31. Guascito MR, Chirizzi D, Malitesta C, Siciliano T, Tepore A (2013) Te oxide nanowires as advanced materials for amperometric nonenzymatic hydrogen peroxide sensing. Talanta 115:863–869
32. Sangeetha NS, Sriman narayanan S (2014) Hydrogen peroxide sensor based on carbon nanotubes-poly (celestine blue) nanohybrid modified electrode. Adv Mater Res 938:263–268
33. Sangeetha NS, Ramaprabhu S, Sriman Narayanan S (2013) Poly (celestine blue)-graphene oxide nanohybrid modified electrode for amperometric determination of hydrogen peroxide. Graphene 1:136–141
34. Brown KR, Walter DG, Natan MJ (2000) Seeding of colloidal au nanoparticle solutions. 2. Improved control of particle size and shape. Chem Mater 12:306–313
35. Torninaga M, Shimazoe T, Nagashima M, Kusuda H, Nkubo A, Kuwahara Y, Taniguchi I (2006) Electrocatalytic oxidation of glucose at gold–silver alloy, silver and gold nanoparticles in an alkaline solution. J Electroanal Chem 590:37–46
36. Ricci F, Amine A, Moscone D, Polleschi G (2003) Prussian blue modified carbon nanotube paste electrodes: a comparative study and a biochemical application. Anal Lett 36:1921–1938
37. Uzunoglu A, Scherbarth AD, Stanciu LA (2015) Bimetallic PdCu/SPCE non-enzymatic hydrogen peroxide sensors. Sens Actuators B 220:968–976
38. Tajabadi MT, Basirun WJ, Lorestani F, Zakaria R, Baradaran S, Amin YM, Mahmoudian MR, Rezayi M, Sookhakian M (2015) Nitrogen-doped graphene-silver nanodendrites for the non-enzymatic detection of hydrogen peroxide. Electrochim Acta 151:126–133
39. Xu F, Deng M, Li G, Chen S, Wang L (2013) Electrochemical behavior of cuprous oxide-reduced graphene oxide nanocomposites and their application in nonenzymatic hydrogen peroxide sensing. Electrochim Acta 88:59–65
40. Heli H, Pishahang J (2014) Cobalt oxide nanoparticles anchored to multiwalled carbon nanotubes: synthesis and application for enhanced electrocatalytic reaction and highly sensitive nonenzymatic detection of hydrogen peroxide. Electrochim Acta 123:518–526

41. Michopoulos A, Kouloumpis A, Gournis D, Prodromidis MI (2014) Performance of layer-by-layer deposited low dimensional building blocks of graphene-prussian blue onto graphite screen-printed electrodes as sensors for hydrogen peroxide. Electrochim Acta 146:477–484
42. Kurowska E, Brzózka A, Jarosz M, Sulka G, Jaskuła M (2013) Silver nanowire array sensor for sensitive and rapid detection of H_2O_2. Electrochim Acta 104:439–447